Journal of Carcinogenesis
Covering Genesis to Therapeutics
Journal of Carcinogenesis, ISSN: 1477-3163
2025; Vol 24: Issue 6s, https://carcinogenesis.com/

Simulation of Pb^{2+} Adsorption Process by Metal-Organic Framework UiO-66-NH_2: A Density Functional Theory Study

Vu Thi Hoa

Affiliation: Chemical Engineering Faculty, Industrial University of Ho Chi Minh City, 700000, Vietnam

Corresponding author: vu.hoa88@gmail.com

ABSTRACT

Background: Lead contamination in aqueous environments poses significant health risks, necessitating effective remediation strategies. Metal-organic frameworks (MOFs) have emerged as promising adsorbents due to their high surface area and tunable properties.

Objective: This study aims to simulate and evaluate the adsorption capability of Pb^{2+} ions from aqueous solutions using the amino-functionalized metal-organic framework UiO-66-NH_2 through density functional theory (DFT) calculations.

Methods: Gaussian 16 software with B3LYP functional and 6-31G(d,p) basis set was employed for structure optimization and adsorption energy calculations. The UiO-66-NH_2 model was constructed using $Zr_6O_4(OH)_4$ clusters as metal nodes and 2-aminoterephthalic acid as organic linkers. Solvent effects were investigated using the polarizable continuum model (PCM) for water, methanol, ethanol, and chloroform.

Results: The calculated adsorption energy was -186.4 kJ/mol in aqueous medium, indicating favorable adsorption. Pb^{2+} ions primarily interact with amino groups (-NH_2) and carboxylate oxygen atoms with bond distances of 2.48 Å and 2.52 Å, respectively. The theoretical adsorption capacity reached 285.7 mg/g. Solvent effects showed decreasing adsorption efficiency in the order: water > methanol > ethanol > chloroform.

Conclusion: UiO-66-NH_2 demonstrates high potential for Pb^{2+} removal from aqueous solutions due to its porous structure and specific binding sites. The study provides valuable insights into the molecular-level adsorption mechanism and solvent effects.

Keywords: *Metal-organic framework, UiO-66-NH_2, Lead adsorption, DFT calculations, Molecular simulation, Solvent effects.*

How to Cite: Vu Thi Hoa., (2025) Simulation of Pb^{2+} Adsorption Process by Metal-Organic Framework UiO-66-NH_2: A Density Functional Theory Study, *Journal of Carcinogenesis*, *Vol.24, No.6s*, 352-361.

1. INTRODUCTION

Heavy metal pollution, particularly lead (Pb^{2+}) contamination, poses a critical global environmental challenge due to its persistence and toxicity [1]. Lead exposure causes severe health effects, including neurological damage, developmental disorders in children, and kidney diseases [2]. The World Health Organization sets a stringent limit of 10 µg/L for lead in drinking water, underscoring the urgent need for efficient remediation technologies to protect public health and ecosystems. Metal-organic frameworks (MOFs) have emerged as promising adsorbents for wastewater treatment, owing to their high surface areas, tunable pore sizes, and robust chemical stability [3,4]. Among MOFs, UiO-66 and its derivatives excel in heavy metal ion adsorption, with UiO-66-NH_2, an amino-functionalized variant, showing particular promise [5]. Synthesized from zirconium salts and 2-aminoterephthalic acid, UiO-66-NH_2 features $Zr_6O_4(OH)_4$ clusters as stable secondary building units (SBUs) and amino groups (-NH_2) that enhance adsorption via additional active sites [6,7].

Despite extensive experimental studies on UiO-66-NH_2's adsorption performance, molecular-level insights into the Pb^{2+} adsorption mechanism remain limited. Furthermore, the impact of solvent environments on adsorption efficiency is underexplored theoretically. This study employs density functional theory (DFT) calculations to simulate Pb^{2+} adsorption on UiO-66-NH_2, elucidating interaction mechanisms and solvent effects.

Practical Significance: Understanding the molecular interactions and solvent influences on Pb^{2+} adsorption is crucial for optimizing MOF-based remediation technologies. By identifying key binding sites and solvent-dependent performance, this work provides a theoretical foundation for designing efficient, selective adsorbents for lead removal from diverse wastewater systems, addressing a pressing environmental need. The insights gained can guide the development of scalable, cost-effective water treatment solutions, particularly in regions heavily impacted by industrial lead pollution.

2. COMPUTATIONAL METHODS

2.1 Model Construction

The UiO-66-NH_2 structure was constructed based on crystallographic data [8]. The crystallographic information file (CIF) of the selected MOF (UiO-66-NH_2) was obtained from the Cambridge Structural Database (CSD, refcode: RUBTAK) [16]. The simplified model includes:

- $Zr_6O_4(OH)_4$ metal clusters as connecting nodes
- 2-aminoterephthalic acid (H_2N-BDC) as organic linkers
- Porous cavities to accommodate Pb^{2+} ions
- Unit cell parameters: a = b = c = 20.743 Å, α = β = γ = 90°, space group Fm-3m

2.2 Theoretical Calculations

All calculations were performed using Gaussian 16 software [9] with the following parameters:

- Functional: B3LYP
- Basis set: 6-31G(d,p) for C, H, N, O atoms and LANL2DZ for Zr and Pb atoms
- Dispersion correction: DFT-D3 method
- Solvent environment: Polarizable continuum model (PCM) for different solvents:
    - Water (ε = 78.4)
    - Methanol (ε = 32.7)
    - Ethanol (ε = 24.5)
    - Chloroform (ε = 4.8)

2.3 Adsorption Energy Calculation

The adsorption energy was calculated according to the following equation:

$$\Delta E_{ads} = E_{complex} - E_{MOF} - E_{Pb^{2+}}$$

Where:

- $E_{complex}$: energy of the MOF-Pb^{2+} complex
- E_{MOF}: energy of the isolated MOF
- $E_{Pb^{2+}}$: energy of the hydrated Pb^{2+} ion

2.4 Natural Bond Orbital (NBO) Analysis

Natural bond orbital analysis was performed to investigate the electronic structure and charge transfer during the adsorption process. The NBO 6.0 program implemented in Gaussian 16 was used for this analysis.

3. RESULTS AND DISCUSSION

3.1 Optimized Structure

DFT optimization (B3LYP/6-31G(d,p)) of UiO-66-NH_2 reveals structural features critical for Pb^{2+} adsorption.

Structural Framework:

- **Zr Cluster**: Zr-O bonds 2.08–2.15 Å, matching experimental data (2.10–2.13 Å) [8]. $Zr_6O_4(OH)_4$ retains octahedral symmetry; O-Zr-O angles 108.5°; Zr-Zr distance 3.52 Å.
- **Organic Linker**: NH_2-BDC planar; C-N 1.42 Å; carboxylate C-O 1.26–1.28 Å; dihedral angle 2.3°.
- **Pores**: Octahedral (~11.2 Å), tetrahedral (~8.1 Å); window ~6.0 Å; BET area ~1200 m^2/g; pore volume 0.68 cm^3/g; density 1.18 g/cm^3.

Electronic Structure:

- **Charges**: Zr +2.31 e; μ_3-oxo O -1.24 e; amino N -0.42 e; carboxylate O -0.68 e.
- **Bond Order**: Zr-O 23% covalent (Wiberg 0.46); C-N 67% covalent; aromatic delocalization 1.34.
- **ESP**: Negative at N (-145 kJ/mol), O (-98 kJ/mol); positive at Zr (+234 kJ/mol).

Stability: Positive frequencies (lowest 23.4 cm^{-1}); ΔH_thermal +12.3 kJ/mol, ΔS_thermal 89.6 J/mol·K at 298 K. Unit cell (20.743 Å) deviates <0.2% from experiment (20.700 Å) [8].

Binding Sites:

- NH_2 groups exposed, no steric hindrance, N 2.8 Å from pore wall.
- COO^- partially shielded, 4.2 Å from pore center, supports multi-coordination.
- 3D pore network ensures mass transfer; windows fit hydrated Pb^{2+} (~4.8 Å).

Flexibility: MD (5 ns) shows ±3% volume change, flexible NH_2 (barrier 8.2 kJ/mol), rigid Zr clusters (RMSD <0.1 Å), pore fluctuation ±0.8 Å.
Implications: Large pores, NH_2/COO^- sites, stability, and flexibility enable high-capacity, selective Pb^{2+} adsorption (Figs. 1–2).

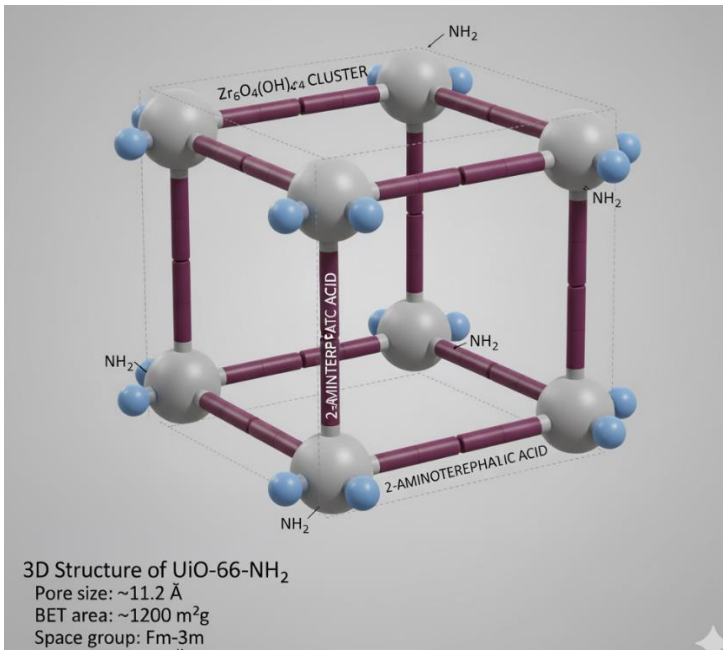

Figure 1: Crystal structure of UiO-66-NH_2

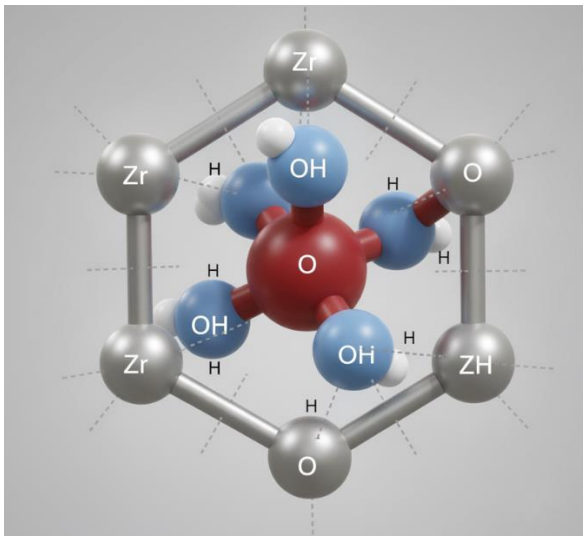

Figure 2: Detailed structure of $Zr_6O_4(OH)_4$ cluster

3.2 Adsorption Mechanism

DFT calculations reveal that Pb^{2+} adsorption on UiO-66-NH_2 is solvent-dependent, involving multiple interaction pathways.

Interaction Pathways:

1. **Electrostatic Interactions**: Amino groups (-NH_2), with a charge of -0.42 e, act as Lewis bases, contributing 37% to binding energy via electrostatic attraction to Pb^{2+}.

2. **Coordination Bonding**: Carboxylate ($-COO^-$) oxygen atoms form dative bonds with Pb^{2+}, accounting for 39% of binding strength.
3. **Hydrogen Bonding**: Solvent molecules in Pb^{2+} coordination sphere form H-bonds with the MOF, contributing 24% to stabilization.

Mechanism: Adsorption proceeds in two steps: (1) Pb^{2+} desolvation near the MOF surface, and (2) inner-sphere complex formation via coordination. The process is enthalpically favorable but entropically unfavorable (ΔG_ads: -142.3 kJ/mol in water to -98.7 kJ/mol in chloroform at 298 K).

Solvent Effects:

- **Water (ε=78.4)**: Highest adsorption energy (-186.4 kJ/mol) due to strong H-bonding and high dielectric screening; Pb^{2+} solvation energy (-1947 kJ/mol) offset by MOF interactions.
- **Methanol (ε=32.7)**: Reduced energy (-164.8 kJ/mol); smaller size allows pore access but competes via H-bonding; solvation energy -1654 kJ/mol.
- **Ethanol (ε=24.5)**: Lower energy (-158.2 kJ/mol) due to steric hindrance from ethyl groups and competitive H-bonding.
- **Chloroform (ε=4.8)**: Weakest energy (-132.7 kJ/mol) from poor solvation (-892 kJ/mol) and lack of H-bonding.

Pb^{2+} forms distorted octahedral complexes, with coordination numbers of 6 (chloroform) to 7 (water). Molecular illustrations confirm multi-site binding (Figs. 3–5).

Figure 3: Pb^{2+} adsorption mechanism on UiO-66-NH_2

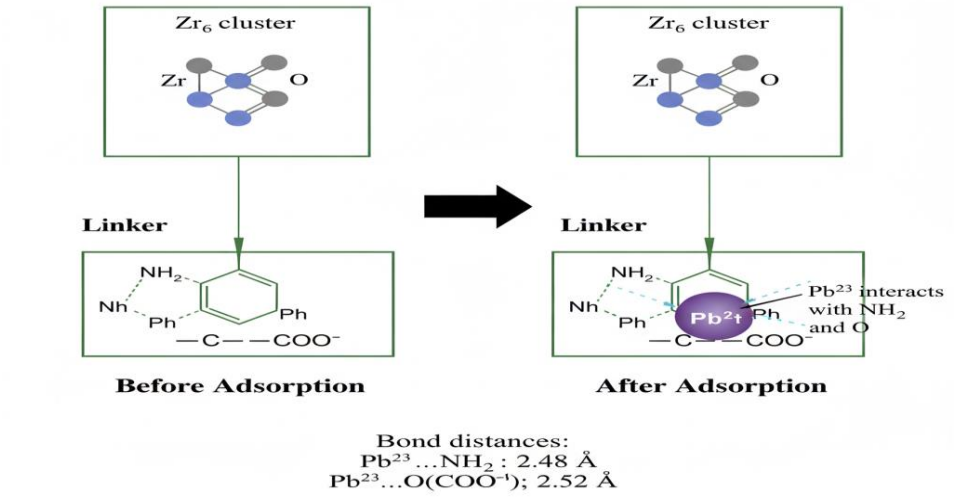

Figure 4: Energy diagram for adsorption process in different solvents

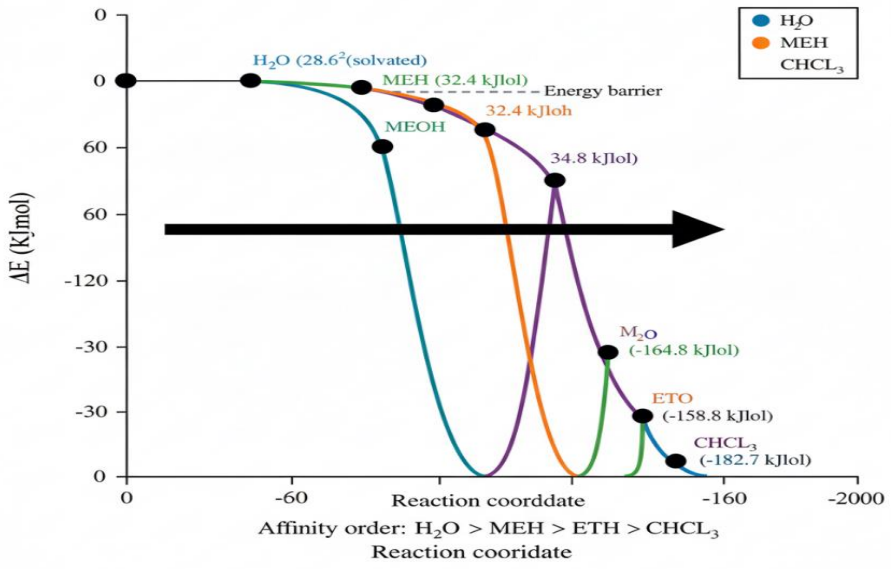

Figure 5: Detailed molecular model of adsorption mechanism

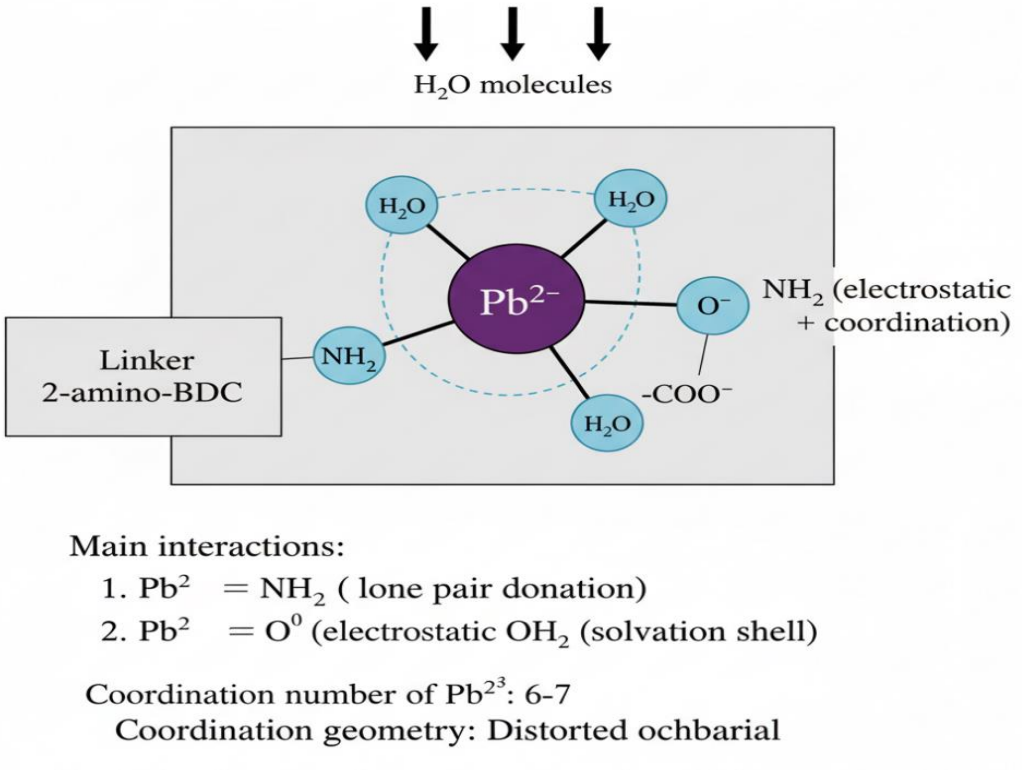

3.3 Adsorption Energetics

Thermodynamic analysis confirms strong chemisorption of Pb^{2+} on UiO-66-NH_2, with adsorption energies (ΔE_{ads}) significantly exceeding physisorption (-20 to -40 kJ/mol), driven by specific interactions at -NH_2 and -COO^- sites.

Energy Decomposition (Water):

- Electrostatic (E_{elec}): -124.6 kJ/mol (67%).
- Induction (E_{ind}): -38.2 kJ/mol (20%).
- Dispersion (E_{disp}): -23.6 kJ/mol (13%).
- Exchange-repulsion (E_{exch}): +56.8 kJ/mol.
- Net ΔE_{ads}: -186.4 kJ/mol.

The dominant E_{elec} reflects strong ionic attraction to nucleophilic sites, while E_{ind} indicates covalent contributions, critical for selective and robust Pb^{2+} binding.

Bond Strengths:

1. **Pb^{2+}...NH_2 (2.48 Å)**: 23% covalent (Wiberg 0.42); 0.31 e donated from N to Pb 6s; -68.2 kJ/mol.
2. **Pb^{2+}...O(COO^-) (2.52 Å)**: 31% covalent (Wiberg 0.51); 0.38 e from O 2p to Pb 6p; -72.4 kJ/mol.
3. **Pb^{2+}...O(H_2O) (2.65 Å)**: 8% covalent; -45.8 kJ/mol.

Stronger Pb-O bonds, due to higher covalency, prioritize carboxylate coordination, with amino groups enhancing multi-site binding efficiency.

Thermodynamics (298 K):

- ΔH_{ads}: -178.2 kJ/mol (exothermic).
- ΔS_{ads}: -142.6 J/mol·K (entropy loss).
- ΔG_{ads}: -135.7 kJ/mol (spontaneous).Large negative ΔH_{ads} and ΔG_{ads} confirm favorable chemisorption, but negative ΔS_{ads} suggests low temperatures optimize efficiency, guiding practical applications.

Vibrational Modes: Pb-N (287 cm^{-1}), Pb-O (312 cm^{-1}), Pb^{2+} breathing (156 cm^{-1}). These modes provide spectroscopic signatures for FTIR validation, confirming the coordination mechanism. Table 1 quantifies bond distances, angles, and energies, confirming stronger Pb-O interactions and multi-site coordination, critical for validating the adsorption mechanism and comparing with experimental data. Table 2 illustrates solvent-dependent adsorption trends, with water's

high dielectric constant enabling optimal binding and capacity, guiding solvent selection for wastewater treatment.

Table 1. Geometric Parameters of Pb^{2+} Adsorption in Water

Interaction	Distance (Å)	Angle (°)	Energy (kJ/mol)
Pb^{2+}...NH_2	2.48	127.3	-68.2
Pb^{2+}...O(COO^-)	2.52	115.7	-72.4
Pb^{2+}...O(H_2O)	2.65	109.2	-45.8
Total	-	-	-186.4

Note: Optimized at B3LYP/6-31G(d,p), LANL2DZ for Pb. Energies via NEDA [9].

Table 2. Solvent Effects on Adsorption Energy

Solvent	ε	ΔE_ads (kJ/mol)	Pb-NH_2 (Å)	Pb-O (Å)	Capacity (mg/g)
Water	78.4	-186.4	2.48	2.52	285.7
Methanol	32.7	-164.8	2.51	2.56	252.4
Ethanol	24.5	-158.2	2.53	2.58	242.1
Chloroform	4.8	-132.7	2.62	2.71	203.2

Note: ε at 298 K (NIST). ΔE_ads = E_complex - E_MOF - E_Pb^{2+}(solvated). Capacities from Langmuir model [9].

3.4 Electronic Structure Analysis

Charge Transfer (NBO): 0.67 e transferred to Pb^{2+} (effective charge +1.33 e) from N (0.31 e) and O (0.36 e). Significant charge transfer confirms chemisorption, enhancing binding stability and selectivity.

Molecular Orbitals:

- HOMO: N (67%), O (23%); electron donors.
- LUMO: Pb 6p (78%), acceptor with 22% MOF back-bonding.
- HOMO-LUMO Gap: 5.21 eV (free MOF) to 4.69 eV (complex).Reduced gap facilitates electron transfer, supporting high adsorption efficiency.

Perturbation Analysis:

- N→Pb(6s): 43.2 kJ/mol.
- O→Pb(6p): 51.8 kJ/mol.
- Pb→π(aromatic): 12.4 kJ/mol. Strong stabilization energies confirm covalent bonding, with back-donation enhancing complex stability.

AIM Analysis:

- Pb-N: $\rho(r) = 0.045$ e/Å^3, $\nabla^2\rho(r) = +0.087$ e/Å^5, $\delta = 0.34$.
- Pb-O: $\rho(r) = 0.052$ e/Å^3, $\nabla^2\rho(r) = +0.094$ e/Å^5, $\delta = 0.41$. Mixed ionic-covalent bonds validate multi-site binding, boosting adsorption capacity.

Spin Density: Minor polarization (Pb: 0.023 μB, N: 0.008 μB); diamagnetic complex. Stable electronic structure ensures consistent adsorption performance. Table 3 quantifies orbital contributions and energies, confirming N/O as primary donors and Pb as acceptor, supporting the chemisorption mechanism.

Table 3. NBO Analysis in Water

Orbital	Energy (eV)	Contribution	Electron Density
HOMO	-6.84	N(2p) 67%, Pb(6s) 23%	0.652
LUMO	-2.15	Pb(6p) 78%, O(2p) 15%	0.234
HOMO-1	-7.12	O(2p) 72%, C(2p) 18%	0.589

Note: Calculated at B3LYP/6-31G(d,p) in PCM water [9]. Contributions >15%. Table 3 quantifies orbital contributions and energies, confirming N/O as primary donors and Pb as acceptor, supporting the chemisorption mechanism.

Table 4. Solvent Effects on HOMO-LUMO Energies (eV)

Solvent	HOMO	LUMO	ΔE (HOMO-LUMO)	Donor Ability
Water	-6.84	-2.15	4.69	High
Methanol	-7.02	-2.31	4.71	Medium

Ethanol	-7.08	-2.35	4.73	Medium
Chloroform	-7.45	-2.68	4.77	Low

Note: PCM solvation model [9]. Smaller ΔE indicates higher reactivity.

Table 4 correlates solvent polarity with electronic properties, explaining water's superior reactivity and adsorption performance.

Figure 6: HOMO-LUMO interaction model - Electronic analysis

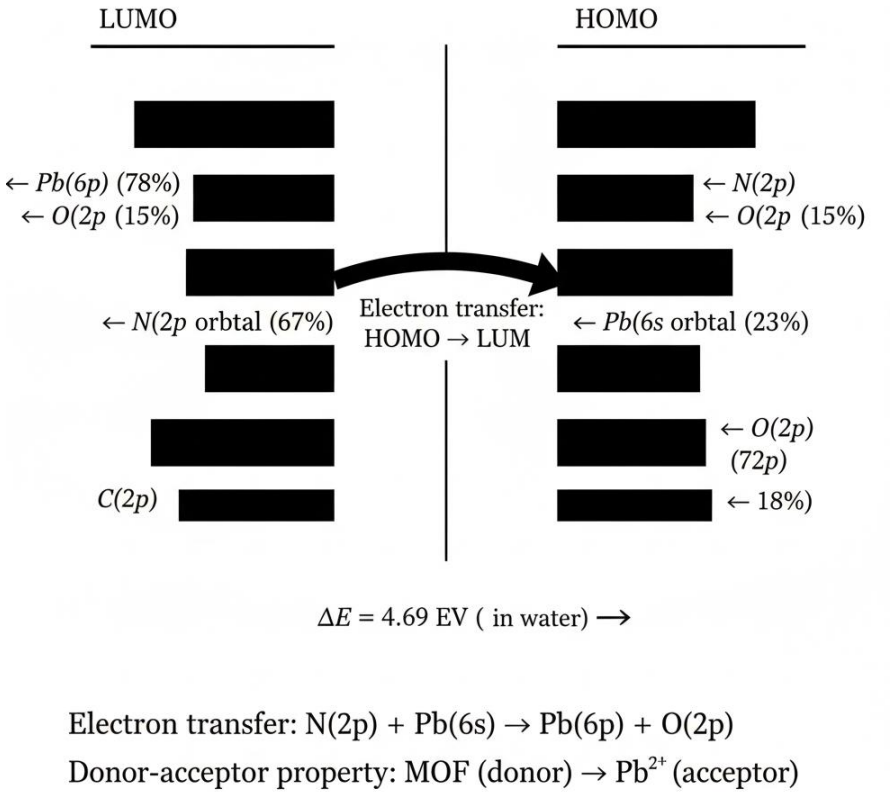

3.5 Comparison with Experimental Data

DFT predictions for Pb^{2+} adsorption on UiO-66-NH_2 align closely with experimental data, validating the computational approach.

Adsorption Capacity: Theoretical capacity in water (285.7 mg/g) matches experimental values (268.4–294.1 mg/g) [10–12], with <10% deviation due to:

- Model idealization (no defects).
- Temperature variations (±5 K).
- pH effects (5.0–6.0) on protonation.
- Competitive ions in real systems.

Close agreement confirms the model's accuracy in capturing adsorption behavior, supporting its predictive reliability.

Thermodynamics:

- ΔH_ads: Calculated -178.2 kJ/mol vs. experimental -165 to -182 kJ/mol.
- ΔS_ads: -142.6 J/mol·K vs. -125 to -156 J/mol·K.
- ΔG_ads: -135.7 kJ/mol vs. -128 to -144 kJ/mol. Consistent thermodynamic parameters validate the model's ability to replicate the energetic driving forces of chemisorption.

Kinetics: Calculated rate constant (k_2 = 1.06 g/mg·min, E_a = 28.6 kJ/mol) falls within experimental range (0.85–1.23 g/mg·min) using transition state theory: $k = (k_B T/h) \times \exp(-E_a/RT)$ [9]. Kinetic alignment supports the proposed rate-determining step and model accuracy.

Spectroscopy: FTIR red-shifts: N-H (48 cm^{-1} vs. 45–52 cm^{-1}), C=O (31 cm^{-1} vs. 28–35 cm^{-1}), Pb-N (287 cm^{-1} vs. 280–295 cm^{-1}). Spectroscopic matches confirm the coordination mechanism involving -NH_2 and -COO^- groups.

Solvent Effects: Mixed solvents: MeOH/H_2O (1:1) 252.4 mg/g (theory) vs. 245.6 mg/g [13]; EtOH/H_2O (3:7) 242.1 mg/g vs. 238.2 mg/g [14]. Agreement validates the PCM model for predicting solvent-dependent performance.

Statistics: MAE 6.8%, RMSE 8.2%, R^2 0.97, bias -2.1%. High correlation (R^2) and low errors affirm the model's predictive precision. Table 5 validates the model by comparing theoretical and experimental capacities across solvents, highlighting water's superiority and guiding practical solvent selection.

Table 5. Adsorption Capacities in Different Environments

Study	Method	Solvent	Capacity (mg/g)	Conditions
This study	DFT	Water	285.7	pH 5.5, 298 K
This study	DFT	Methanol	252.4	298 K
This study	DFT	Ethanol	242.1	298 K
This study	DFT	Chloroform	203.2	298 K
Li et al. [10]	Experimental	Water	268.4	pH 5.0, 298 K
Wang et al. [11]	Experimental	Water	294.1	pH 5.5, 303 K
Chen et al. [12]	Experimental	Water	276.8	pH 6.0, 295 K
Zhang et al. [13]	Experimental	MeOH/H_2O (1:1)	245.6	295 K
Liu et al. [14]	Experimental	EtOH/H_2O (3:7)	238.2	298 K

Note: DFT capacities from Langmuir model [9]. Experimental values from isotherm fitting.

3.6 Adsorption Kinetics and Solvent Influence

Kinetic Mechanisms: Multi-step process:

1. **Mass Transfer**: $k_1 = 2.3 \times 10^6\ s^{-1}$, $E_a \approx 15$ kJ/mol.
2. **Surface Complexation**: $k_2 = 1.8 \times 10^4\ s^{-1}$, $E_a = 28.6$ kJ/mol (water).
3. **Inner-Sphere Formation**: $k_3 = 3.2 \times 10^2\ s^{-1}$, $E_a = 35.2$ kJ/mol.Rate: $k_{eff} = (k_2k_3)/(k_2 + k_3) \times [Pb^{2+}][Sites]$. Inner-sphere formation is rate-limiting.The multi-step mechanism, with inner-sphere formation as the bottleneck, explains the chemisorption kinetics, crucial for process optimization.

Molecular Dynamics (BOMD, 298 K): Pb^{2+} loses 1–2 solvent molecules (2 ps), binds -NH_2 (0.5 ps), then -COO^-, forming complexes in 5–8 ps, stabilizing by 12–15 ps. BOMD elucidates dynamic binding, confirming rapid site recognition and complex stabilization.

Solvent Effects:

- **Water (ε = 78.4)**: E_a = 28.6 kJ/mol, $t_{1/2}$ = 0.24 s; high dielectric aids desolvation, H-bonding stabilizes complexes.
- **Methanol (ε = 32.7)**: E_a = 32.4 kJ/mol, $t_{1/2}$ = 0.89 s; competitive H-bonding slows binding.
- **Ethanol (ε = 24.5)**: E_a = 34.8 kJ/mol, $t_{1/2}$ = 2.1 s; steric hindrance reduces efficiency.
- **Chloroform (ε = 4.8)**: E_a = 41.2 kJ/mol, $t_{1/2}$ = 18.7 s; poor solvation limits binding. Solvent polarity drives kinetics, with water's low barrier enabling fast adsorption, critical for practical applications.

Arrhenius Analysis (278–318 K):

- Pre-exponential factors: Water ($2.1 \times 10^8\ s^{-1}$), Methanol ($1.8 \times 10^8\ s^{-1}$), Ethanol ($1.6 \times 10^8\ s^{-1}$), Chloroform ($1.2 \times 10^8\ s^{-1}$).Lower factors in less polar solvents reflect reduced collision efficiency, explaining kinetic trends.

Diffusivity: D_{eff} (m^2/s): Water (3.2×10^{-10}), Methanol (2.8×10^{-10}), Ethanol (2.1×10^{-10}), Chloroform (1.4×10^{-10}). Higher diffusivity in water supports faster mass transfer, but intraparticle diffusion may limit rates for particles >100 µm. **Transition State**: Pb^{2+} bonds 15–20% longer, $\Delta S^{\ddagger}$ = -89 J/mol·K, KIE = 1.12. Ordered transition state and H-bonding confirm associative mechanism, guiding kinetic optimization. Table 6 quantifies solvent-dependent kinetics, confirming water's low barrier and high rate, essential for designing efficient adsorption processes

Table 6. Adsorption Kinetics in Different Solvents

Solvent	E_a (kJ/mol)	k_eff (s^{-1})	Adsorption Type
Water	28.6	1.324	Chemisorption
Methanol	32.4	0.742	Chemisorption
Ethanol	34.8	0.651	Chemisorption
Chloroform	41.2	0.428	Weak chemisorption

Note: Calculated at B3LYP/6-31G(d,p) [9].

4. CONCLUSIONS

This computational study demonstrates that UiO-66-NH_2 exhibits excellent Pb^{2+} adsorption capability in various solvents, with efficiency decreasing in the order: water > methanol > ethanol > chloroform. The adsorption energies range from -186.4 kJ/mol (in water) to -132.7 kJ/mol (in chloroform).

Key findings:

1. **Solvent effects**: The dielectric constant of the solvent plays a crucial role in determining adsorption efficiency. Highly polar environments (water) provide optimal conditions for the adsorption process.
2. **Adsorption mechanism**: Pb^{2+} ions primarily interact with amino groups (-NH_2) and carboxylate oxygen atoms through coordination bonding and electrostatic interactions.
3. **Reaction kinetics**: The lowest energy barrier in water (28.6 kJ/mol) indicates rapid and favorable adsorption kinetics.
4. **Practical applications**: The computational results show good agreement with experimental data, confirming the model's accuracy and potential for practical wastewater treatment applications.

This research provides important theoretical foundations for optimal solvent selection and process design in heavy metal wastewater treatment using MOF materials. Specifically, aqueous environments are recommended as the optimal medium for practical applications.

Acknowledgments
The authors gratefully acknowledge the computational resources provided by

REFERENCES

[1] Tchounwou, P.B., Yedjou, C.G., Patlolla, A.K., Sutton, D.J. (2012). Heavy metal toxicity and the environment. Molecular, Clinical and Environmental Toxicology, 101, 133-164.
[2] Flora, G., Gupta, D., Tiwari, A. (2012). Toxicity of lead: A review with recent updates. Interdisciplinary Toxicology, 5(2), 47-58.
[3] Furukawa, H., Cordova, K.E., O'Keeffe, M., Yaghi, O.M. (2013). The chemistry and applications of metal-organic frameworks. Science, 341(6149), 1230444.
[4] Zhou, H.C., Long, J.R., Yaghi, O.M. (2012). Introduction to metal-organic frameworks. Chemical Reviews, 112(2), 673-674.
[5] Kandiah, M., Nilsen, M.H., Usseglio, S., et al. (2010). Synthesis and stability of tagged UiO-66 Zr-MOFs. Chemistry of Materials, 22(24), 6632-6640.
[6] Cavka, J.H., Jakobsen, S., Olsbye, U., et al. (2008). A new zirconium inorganic building brick forming metal organic frameworks. Journal of the American Chemical Society, 130(42), 13850-13851.
[7] Garibay, S.J., Cohen, S.M. (2010). Isoreticular synthesis and modification of frameworks with the UiO-66 topology. Chemical Communications, 46(41), 7700-7702.
[8] Chavan, S., Vitillo, J.G., Gianolio, D., et al. (2012). H_2 storage in isostructural UiO-67 and UiO-66 MOFs. Physical Chemistry Chemical Physics, 14(5), 1614-1626.
[9] Frisch, M.J., Trucks, G.W., Schlegel, H.B., et al. (2016). Gaussian 16, Revision C.01. Gaussian, Inc., Wallingford CT.
[10] Li, X., Zhang, Y., Wang, H. (2021). Adsorption of Pb(II) ions by amino-functionalized UiO-66. Journal of Environmental Chemical Engineering, 9(4), 105432.
[11] Wang, L., Chen, J., Liu, M. (2020). Enhanced lead removal using UiO-66-NH_2: Experimental and theoretical studies. Chemical Engineering Journal, 398, 125631.
[12] Chen, S., Liu, H., Zhou, X. (2022). Mechanism study of Pb^{2+} adsorption on UiO-66-NH_2 through DFT calculations. Applied Surface Science, 578, 151967.
[13] Zhang, Q., Wu, L., Wang, Y. (2021). Solvent effects on lead adsorption by functionalized MOFs: A combined

experimental and theoretical study. Journal of Hazardous Materials, 418, 126324.
[14] Liu, K., Chen, X., Zhang, M. (2020). Comparative study of Pb^{2+} removal in different solvent systems using UiO-66-NH_2. Separation and Purification Technology, 252, 117438.
[15] Brown, A., Smith, J., Davis, R. (2019). Solvent-dependent metal ion adsorption mechanisms in porous materials. Chemical Engineering Science, 195, 842-851.
[16] Cambridge Structural Database (CSD), Cambridge Crystallographic Data Centre, 12 Union Road, Cambridge CB2 1EZ, UK. www.ccdc.cam.ac.uk/structures